RESEARCH NOTE

MODELING OF UNREINFORCED AND REINFORCED PAVEMENT COMPOSITE MATERIAL USING HISS MODEL

Praveen Aggarwal*

Department of Civil Engineering, NIT
Kurukshetra, India
Praveen_agg1@rediffmail.com

K. G. Sharma and K. K. Gupta

Department of Civil Engineering, IIT
Delhi, India
kgsharma@civil.iitd.ac.in - kkg@civil.iitd.ac.in

*Corresponding Author

(Received: September 23, 2006 – Accepted in Revised Form: March 18, 2007)

Abstract With the advent of high strength geogrids, the interest of civil engineers in using geosynthetics as reinforcement material in pavement construction has increased. An experimental study is carried out at IIT Delhi to understand the effect of geogrid in unpaved roads. Behavior of composite material, which comprises of Yamuna sand as subgrade and Water Bound Macadam (WBM) as base course is studied with and without geogrid reinforcement under drained conditions. A geogrid is used as reinforcing material. Drained triaxial tests were performed at three different confining pressures of 50, 100 and 200 kPa on both unreinforced composite and reinforced composite materials of specimen size 100mm diameter and 200mm height. Hierarchical single surface (HISS) model developed by Desai and co-workers is used to model the unreinforced and reinforced composite material. A computer program PARA6 is used to calculate the various parameters and to back predict the stress-strain-volume change behavior of unreinforced and reinforced composite materials. The predicted results match closely with the observed results.

Keywords Geosynthetics, WBM, Composite Material, HISS Model

چکیده با پیدایش شبکه های مسلح کننده مقاوم خاک، نظر مهندسین عمران به کاربرد بیشتر ژئوسنتز به عنوان یک مصالح مسلح کننده در ساخت روسازی ها جلب شده است. یک تحقیق تجربی در ایـن زمینـه در دانـشگاه IIT دهلی در جهت درک بهتر اثر این شبکه ها در راه های بدون روسازی صورت پذیرفته است. در این تحقیـق رفتار چنین مصالح مرکب که متشکل از ماسه یامونا به منزله زیر اساس و ماک آدام آب خورده (WBM) به منزله لایه اساس درشت در دو حالت با شبکه مسلح کننده و بدون آن به صورت زهکشی شـده مـورد ارزیـابی قـرار گرفته است. شبکه به کار رفته در این مورد نقش مسلح کننده مصالح دانه ای را به عهده داشته است. آزمایشهای سه محوری زهکشی نیز در محدوده فشارهای ۵۰، ۱۰۰ و ۲۰۰ کیلو پاسکال بر مواد مرکب مسلح و غیر مـسلح دارای ۱۰۰ میلی متر قطر و ۲۰۰ میلی متر ارتفاع انجام شده و با الگوی رفتاری هیرآرکی با سطح یگانـه (HISS) ارائه شده توسط آقای دسای و همکارانش در جهت رفتار سنجی مواد به کـار گرفتـه شـده اسـت. یـک برنامـه کامپیوتری به نام PARAG برای ارزیابی فراسنج های مختلف در اجرای تطبیق اولیه رفتار تـنش-کـرنش-تغییـر حجم مصالح مرکب مسلح و غیر مسلح مورد استفاده قرار گرفته است. نتایج حاصله با نتـایج مـشاهداتی تطبیـق نزدیکی داشته است.

1. INTRODUCTION

Pavement is a structure made in between the wheel and the natural ground. The basic aim of pavement is to provide a hard surface for the movement of wheels without significant deformation and to distribute the wheel load effectively to a larger area of natural ground so that the stresses are within bearing capacity. Temporary or unpaved roads with low traffic volume are required for construction and access roads, contractors' haul roads, short-term detours, for example, bridge replacement construction etc. Further, such roads are also frequently constructed world wide to support resource industry viz. forestry, mining, oil and tar-sand extraction, agriculture and others.

Considering the economic significance of unpaved roads, attempts have been made to understand their behavior, so that the benefit of geosynthetic can be quantified. Initially low strength geotextiles were used as a separation layer only, thereby maintaining the effective thickness. Reinforcement function of geosynthetics was realized with the emergence of improved materials in the form of strong woven geotextile and geogrids. Various factors, which affect the behavior of soils, include soil density, confining pressure, drainage conditions and the stress path followed triaxial testing. In the analysis load deformation problem, stress-strain relationship plays an important role. Reinforced soils have further complex behavior due to insertion of reinforcement layer. The behavior is dependent on many additional factors such as the quantity, type, spacing, interface properties and tensile strength of the reinforcement. Stress-strain relationship of the reinforced soil is thus a function of these factors in addition to the other factors of unreinforced soil.

A number of experimental and analytical studies have been undertaken by researchers to understand the behavior of the reinforced soils. Interface friction behavior is experimentally studied by modified direct shear test and/or pullout test. Stress-strain and strength characteristics have been studied mostly by conducting triaxial tests.

Triaxial tests were conducted on cylindrical specimen of reinforced sand using woven fabric glass netting as reinforcement [1]. It was observed that the axial stress increased with the number of reinforcement layers. Axial strain at failure also increased due to insertion of the reinforcement. Strength of the reinforced soil was observed to be increasing with the number of reinforcement layers. The beneficial effects of reinforcing subgrade soils with a single layer of geogrid and their behavior under static and cyclic loading were also investigated by other researchers [2] and were observed that geogrids can play an important role in the control of the rut formation in pavements. Comprehensive statistical analyses were conducted on the collected triaxial test data [3]. The results of these analyses indicated that the geogrid inclusion within crushed limestone samples significantly reduced their permanent deformations and it was also observed that this improvement was significantly affected by the geogrid stiffness.

Constitutive model is a mathematical relation, which reproduces the observed response of a continuous medium. Constitutive models can be broadly classified into the following three categories.

- Empirical models
- Elasto-plastic models
- Elasto-viscoplastic models

All geological materials show plasticity almost from the beginning. Therefore, stress-strain and volume change response of many geologic media including water bound macadam, bituminous concrete can only be predicted by plasticity models. Some of the yield criteria are

- Mohr-Coulomb Criterion
- Drucker-Prager Yield Criterion
- Critical State Models
- HISS model

Two models, the SIGMA-model and TAU-model were postulated using Yang's results for describing the strength of soil mass reinforced with horizontal layers [4]. A semi-empirical formula is suggested by Broms [5] to evaluate the strength of reinforced soil in a triaxial test. He further observed that placement of reinforcement plays an important role in the behavior of reinforced soils. The empirical relation was, however, very complex. An attempt was made by [6] to model the results with a hyperbolic model. All these studies were conducted using the conventional triaxial compression stress path. Baykal et al. [7] conducted triaxial tests using two stress paths and observed that stress-strain behavior of reinforced soil is stress path dependent. Soni [8] studied the behavior of reinforced soil using six stress paths and modeled the behavior using HISS model.

In the present study a series of drained triaxial tests were performed on unreinforced and geogrid reinforced composite specimens (Water Bound Macadam and Yamuna sand), and their stress-strain and volume change behavior is modeled using the Hierarchical Single Surface model. Modeled stress-strain and volume change behavior are compared with the experimentally observed behavior, and were found in close agreement.

2. ROLES OF GEOSYNTHETICS IN UNPAVED ROADS

The use of geosynthetics in the pavement construction started to serve as a separation layer. An example of use of geosynthetics as a separation layer is in the construction of an airfield in Switzerland [9]. With the development of new stronger geosynthetics reinforcement application of this new construction material became apparent. Today geosynthetics are used in the pavement construction primarily to serve the following four functions:

- Separation
- Filtration
- Drainage
- Reinforcement

2.1. Behavior of Reinforced Flexible Pavement

The strengthening effect of geosynthetics in flexible pavement has been studied through plate bearing tests on laboratory models and through triaxial tests under static and repeated loading.

According to [10] non-woven geotextile inhibits the punching type failure characteristics of soft soil by restraining the soft subgrade and they proposed to use higher bearing capacity factors in reinforced system (irrespective of the mechanical properties of geotextiles).Similar observations were made in a test road with non-woven geotextile [11].

Later on [12-13] indicated that the performance of such systems improved with modulus of geotextiles and led to the inclusion of membrane effect in theoretical analysis and design procedures proposed by [14-16]. [17] proposed the restraint action of geotextiles on the aggregate layer.

Limited studies have been done on reinforced pavement system under repeated loading. From the above literature it is very clear that a geotextile effectively reduces the permanent deformation of the reinforced pavement system. The beneficial effect of the geotextile in controlling the evolution of permanent deformation appears to be due to the following reasons as quoted by [18-19]

- Geotextile at the interface improves the load spreading capacity of the aggregate consequently the stress-strain state in the subgrade changes leading to less plastic strain with particular number of load repetitions.
- Lateral restraint effect of geotextile restricts and the lateral movement of the subgrade soil away from the directly loaded zone.

With the increase in thickness of the aggregates the beneficial effect decreases. For better performance some lateral extensions beyond the directly loaded area is also essential [19]. On the other hand, [20] found that anchorage details of geotextile do not affect the behavior of unpaved road models.

The cumulative permanent and elastic deformations at the surface under repetitive load tests on aggregate-soil system with and without reinforcement at the interface are observed by [21]. From the results it is concluded that under similar test conditions geosynthetics can reduce the elastic deformation on such systems, thereby improving the resilient modulus of the system.

3. HISS MODEL

In the present study HISS model is used. Classical plasticity-based models (von Mises, Mohr Coulomb and Drucker-Prager) can provide satisfactory responses for some geological materials, but in general they do not predict the observed behavior accurately, particularly the volume change response during plastic deformations near failure. Models based on critical state and cap approaches suffer from various limitations such as: (i) the failure and cap surfaces intersect which may cause computational difficulties; (ii) dilative plastic strains are predicted only at failure, while many geological materials experience dilative strains before the peak is reached; (iii) the yield strength is assumed to be the same for all stress paths, while many geological materials possess different strengths for different stress paths; and (iv) the hardening is dependent on volumetric plastic strains, while deviator plastic strains can also affect hardening.

The Hierarchical Single Surface (HISS) models (δ_0 and δ_1) are proposed by Desai [22] and modified by Desai and co-workers [23]. The non-associative (δ_1) model has been adopted for the present study for the prediction of stress-strain-volume change behavior of soil and water bound macadam. The models were developed using the theory of elasto-plasticity and are capable of taking care of various complexities such as stress path dependency, non-associativeness and anisotropy. In these models, a unique and continuous yield function is used that leads to failure when an ultimate condition is reached. The brief description of the model is as follows.

The constitutive equation for elasto-plasticity can be written as

$$d\sigma_{ij} = C^{EP}_{ijkl}\, d\varepsilon_{kl} \tag{1}$$

where C^{EP}_{ijkl} is the constitutive matrix for elasto-plastic approach.

The yield function for δ_0 model is given as

$$F = \left(\frac{J_{2D}}{P_a^2}\right) - \left[-\alpha\left(\frac{J_1}{P_a}\right)^n + \gamma\left(\frac{J_1}{P_a}\right)^2\right](1-\beta S_r)^m \tag{2}$$

$$S_r = \text{Stress ratio} = \frac{\sqrt{27}}{2}\frac{J_{3D}}{J_{2D}^{1.5}} \tag{3}$$

where:

J_1	First invariant of stress tensor
J_{2D}	Second invariant of deviatoric stress tensor
J_{3D}	Third invariant of deviatoric stress tensor
P_a	Atmospheric pressure
α, β, n and γ	Material constants
m	-0.5 For geological materials [23]

For non-associative model δ_1, plastic potential function Q is defined as a modification of F with α replaced by α_Q, i.e.,

$$Q = \left(\frac{J_{2D}}{P_a^2}\right) - \left[-\alpha_Q\left(\frac{J_1}{P_a}\right)^n + \gamma\left(\frac{J_1}{P_a}\right)^2\right](1-\beta S_r)^m \tag{4}$$

where:

$$\alpha_Q = \alpha + \kappa(\alpha_0 - \alpha)(1 - r_v) \tag{5}$$

in which κ is non-associative parameter, α_0 is α at the beginning of shear loading and $r_v = \frac{\xi_v}{\xi}$, ξ_v is volumetric part of ξ (plastic strain trajectory).

3.1 Properties of The Hiss Yield Function

Some of the features of HISS model are as follows:

- The model involves only one continous surface which describes yield or loading surfaces by a single function and also describe the ultimate behaviour. In the model only two parameters γ and β (at ultimate) are used to define the traditional failure.
- Entire hardening and ultimate behaviour is defined by only one function.
- The plot of yield function F is continous and convex in the stress space for geological material. However it intersects the J_1 axis at right angles, as a result it can be implemented in the context of the classical theory of plasticity.
- As the intersection of two or more surfaces and corner in Π plane are avoided, the model is easier to implement in numerical analysis.
- A single parameter growth function α can simulate hardening and include the effect of stress path, volume change and coupling of shear and volumetric responses.

4. DETERMINATION OF MATERIAL CONSTANTS

The HISS model requires nine parameters for the constitutive modeling of any material, which can be classified into five categories.

- Elastic constants (E,ν)
- Ultimate parameters (γ,β,m)
- Phase change parameter (n)
- Hardening parameters (a_1,η_1)
- Non-associative parameter (κ)

The procedure for calculating material parameters has been described in detail in various references [24-27]. It is briefly presented herein.

- Elastic constants (E,ν)

The two elastic constants for an isotropic material, Young's modulus, E and Poisson's Ratio, ν are determined from the average slopes of the initial part of the stress-strain curves and the ratio of lateral and axial strains respectively. Janbu's relation is used to correlate Young's modulus with confining pressure.

$$E = kP_a \left[\frac{\sigma_3}{P_a} \right]^N \tag{6}$$

where k and N are constants.

- Ultimate parameters (γ,β,m)

For many geological materials m is found to be-0.5 [23]. Therefore, in the present work, m is considered as-0.5. The procedure adopted for the calculation of γ and β from the laboratory results is described below.

At the ultimate state, the value of α tends to zero thus, the yield surface degenerates to an open surface-intersecting J_1 axis at infinity. Applying the condition to the yield function, Equation 2, the slope of the ultimate line is derived as

$$\frac{J_1}{\sqrt{J_{2D}}} = \left[\frac{\left(1 - \beta S_r\right)^{1/2}}{\gamma} \right]^{1/2} \tag{7}$$

where: $S_r = 1$ for compression path and $S_r = -1$ for extension path. The ultimate parameters can be found out by conducting the least square fitting procedure on Equation 7 for at least two triaxial tests on $J_1 - \sqrt{J_{2D}}$ plane.

- Phase change parameter (n)

The phase change parameter, n, is calculated using the zero plastic volume change condition, $\frac{\partial F}{\partial J_1} = 0$. An average of n values for different tests is taken as an overall value of n for the material.

- Hardening parameters (a_1,η_1)

In the present study, an isotropic hardening rule was used. The growth function α as suggested by Wathugala [28] is

$$\alpha = \frac{a_1}{\xi^{\eta_1}} \tag{8}$$

Taking natural log on both sides of Equation 8 gives,

$$\ln(\alpha) = \ln(a_1) - \eta_1 \ln(\xi) \tag{9}$$

a_1 and η_1 are determined from the least square fitting procedure for each test. The average value of a_1 and η_1 from various tests are taken as overall values of the hardening parameters.

- Non-associative parameter (κ)

Non-associative parameter, κ in the plastic potential formation, Q is assumed as constant and is determined from the conditions near the ultimate. Basic steps in evaluating κ are given below.

From the flow rule,

$$d\varepsilon_{ij}^p = \lambda \frac{\partial Q}{\partial \sigma_{ij}} \tag{10}$$

we get

$$d\varepsilon_v^p = \lambda \left[\frac{\partial Q}{\partial J_1} \frac{\partial J_1}{\partial \sigma_{11}} + \frac{\partial Q}{\partial J_1} \cdot \frac{\partial J_1}{\partial \sigma_{22}} + \frac{\partial Q}{\partial J_1} \cdot \frac{\partial J_1}{\partial \sigma_{33}} \right] \tag{11}$$

or

$$d\varepsilon_v^p = 3\lambda \frac{\partial Q}{\partial J_1} \tag{12}$$

$$\left(\frac{d\varepsilon_v^p}{d\varepsilon_{11}^p}\right) = \frac{\left(3\frac{\partial Q}{\partial J_1}\right)}{\left(\frac{\partial Q}{\partial \sigma_{11}}\right)} = \nu^p \quad (13)$$

Then from Equation 5,

$\kappa = (\alpha_Q - \alpha) / [(\alpha_0 - \alpha)(1 - r_v)]$

where

$d\varepsilon_{11}^p$	is the axial plastic strain increment,
σ_{11}	is the axial stress, and
$d\varepsilon_v^p$	is the volumetric plastic strain increment.

The ratio of $\frac{d\varepsilon_v^p}{d\varepsilon_{11}^p}$ can be obtained from the slope of the observed $d\varepsilon_{11}^p$ versus $d\varepsilon_v^p$ response by choosing a point in the ultimate state. Knowing $\frac{d\varepsilon_v^p}{d\varepsilon_{11}^p}$, the value of '$\alpha_Q$' can be calculated using Equation 13 as 'Q' is expressed in terms of 'α_Q'. This value of 'α_Q', along with 'α' and 'r_v' at the ultimate condition, is used to calculate the average value of 'κ'.

Even though, κ could be calculated for any stress point, the portion of ε_v-ε_1 curve near the ultimate condition is used since the deviation (α_Q-α) is the greatest in the ultimate zone. The value of κ has been calculated using the program PARA6.

5. TEST PROGRAM

In order to model the reinforced and unreinforced unpaved composite materials, a series of drained triaxial tests were carried out on unreinforced and reinforced unpaved composite materials at three confining pressures of 50, 100 and 200 kPa.

5.1. Materials

5.1.1. Subgrade soil The subgrade soil used in the present study is Yamuna Sand. Yamuna Sand is locally available sand obtained from the bed of river Yamuna River. The characteristics of Yamuna sand are summarized in Table 1.

5.1.2. Aggregates Crushed stone coarse aggregates and screening were used to prepare the Water Bound Macadam (WBM) mix. The particle size distribution of the coarse aggregate and screening are shown in Figure 1.

Water Bound Macadam (WBM) Mix Design

Water Bound Macadam mix was designed as per [29] specification, for possible use as surfacing course. Delhi Silt (P. I. = 6%) was used as a binding material. Required quantity of both the

TABLE 1. Characteristics of Yamuna Sand.

Property	Value
% Sand	94
% Silt	6
Specific Gravity (SG)	2.67
Coefficient of Uniformity C_u	2.24
Coefficient of Curvature C_c	1.14
Maximum Dry Density ($\gamma_{d\ max.}$)	16 kN/m^3
Minimum Dry Density ($\gamma_{d\ min.}$)	13 kN/m^3

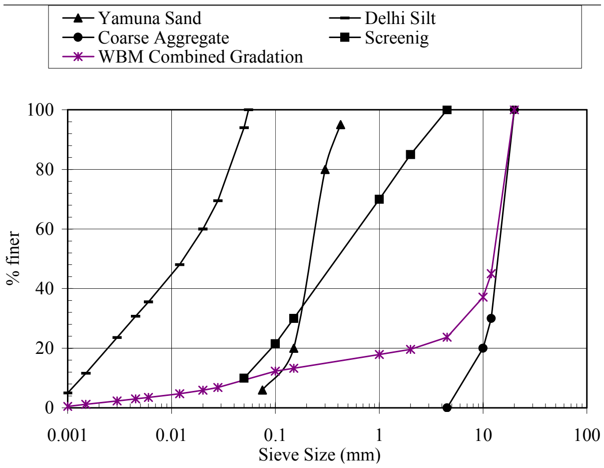

Figure 1. Gradation of yamuna sand, delhi sit, coarse aggregate and screening.

coarse aggregate and screening were mixed with binding material in the ratio of 1.0: 0.16: 0.15 by volume in a loose state under dry conditions. Then the Proctor Compaction Test was carried out to find out the Optimum Moisture Content (OMC) and Maximum Dry Density (MDD) for further use. OMC for WBM is 6.8 % and MDD achieved at this moisture content is 22.30 kN/m^3.

5.1.3. Geogrid The geogrid used was an extruded mesh with an aperture size of 7.1×7.1mm, thickness 1.85mm and at joint is 3.25mm.The wide width tension tests were carried out as per [30] to determine the load deformation behavior in the machine and cross directions of the geogrid. Tensile strength is 7.11 and 6.43 kN/m in the machine and cross directions respectively at 40mm elongation.

5.2 Testing

5.2.1. Triaxial test Conventional triaxial apparatus [31] was used for the triaxial tests. A perspex triaxial cell capable of withstanding more than 1 MPa and with the facility of 100 mm diameter and 200 mm height was used. Thickness of subgrade (Yamuna sand) and base coarse layer (WBM) is 100mm each in both unreinforced and reinforced specimen. Axial strains, deviator stresses and volumetric strains were observed during the tests. It is observed that the mode of failure of unreinforced composite material is by bulging of the subgrade layer, hence reinforcement is provided at the center of the subgrade layer in reinforced composite material specimen (Figure 2). The experimentally observed behavior is presented in Figures 3-6.

From Figure 3 and 5 it is observed that maximum octahedral stress are 213, 501 and 896 kPa at a confining pressure of 50, 100 and 200kPa in an unreinforced composite specimen. With the inclusion of single layer geogrid at the center of the subgrade the peak stresses increases to 265, 597 and 1025 kPa respectively in confining pressure of 50, 100 and 200 kPa. Resulting in an increase in peak stress of 24 %, 19 % and 14 % for a confining pressure of 50, 100 and 200 kPa respectively. This indicates that the benefit of inclusion of the geogrid is more predominant at low confining pressure than higher confining pressure. It is further observed that strain corresponding to peak stress increases with increase in confining pressure, from 5.4 % to 6.15 % in case of unreinforced specimen and 6.3 to 7.2 % in reinforced composite specimen, for a confining pressure of 50 to 200 kPa. From the above observation it can be concluded that inclusion of the geogrid results in an increase in strain corresponding to peak stress at a particular confining pressure.

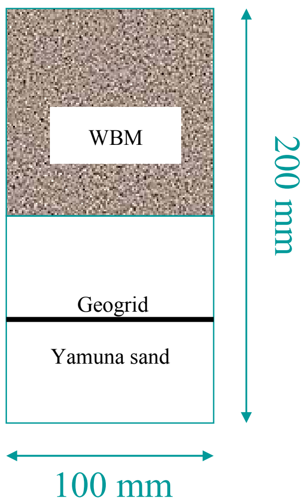

Figure 2. Geogrid reinforced triaxial specimen.

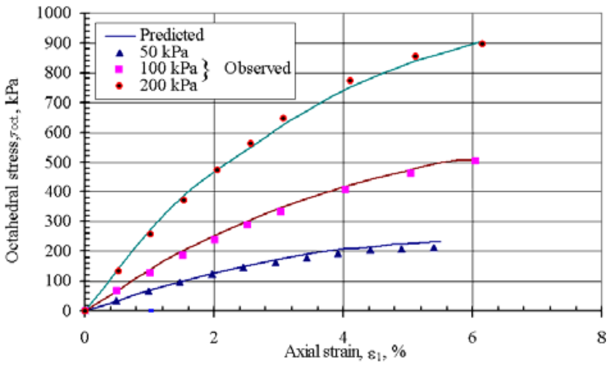

Figure 3. Variation of octahedral stress with axial strain for unreinforced composite material at σ_3 = 50, 100 and 200 kPa.

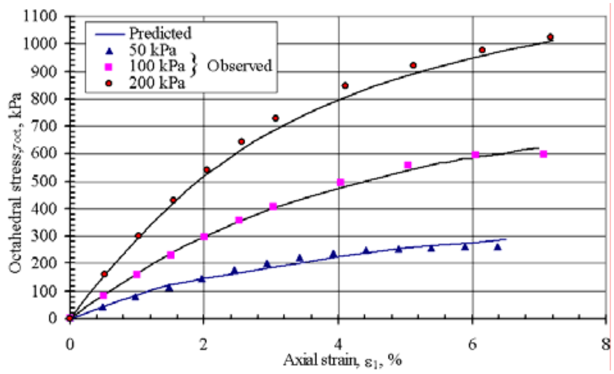

Figure 5. Variation of octahedral stress with axial strain for reinforced composite material at σ_3 = 50, 100 and 200 kPa.

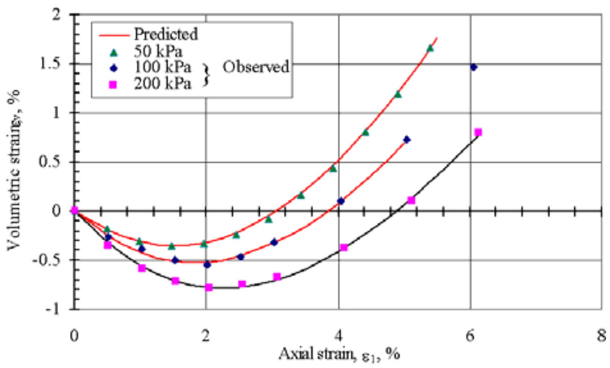

Figure 4. Variation of volumetric strain with axial strain for unreinforced composite material at σ_3 = 50, 100 and 200 kPa.

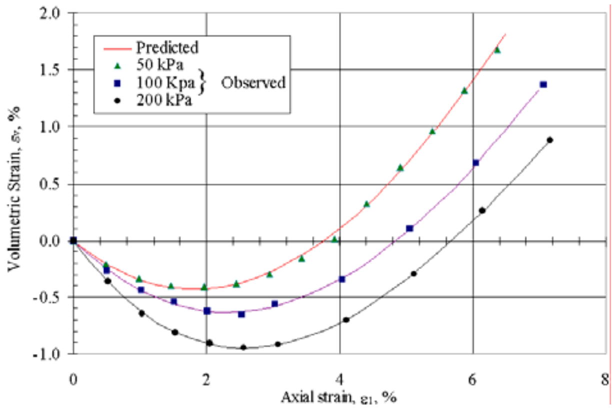

Figure 6. Variation of volumetric strain with axial strain for reinforced composite material at σ_3 = 50, 100 and 200 kPa.

6. PREDICTION

The incremental constitutive relation (Equation 1) has been used to predict the stress-strain-volume change response. The equation is integrated starting from the initial hydrostatic state. The prediction is made using the nine parameters calculated for unreinforced and reinforced composite material under strain control conditions. Both predicted and experimentally observed octahedral stress and volumetric strain with axial strain are presented in Figures 3-4 for the unreinforced case and in Figures 5-6 for the reinforced case. The observed and predicted behavior matches closely.

7. MODELLING

All the nine constants for HISS model are calculated for both unreinforced and reinforced cases and are presented in Table 2.

8. CONCLUSIONS

From the results it is observed that inclusion of geogrid improves the performance of composite material by more than 15 %. Dilation starts at a higher axial strain in the case of reinforced composite material as compared to unreinforced

TABLE 2. The Material Parameters for Unreinforced and Reinforced Composite Materials.

Constant	Unreinforced	Reinforced
k	141.97	171.58
N	1.1280	1.0996
γ	0.0798	0.0840
β	0.74	0.74
m	-0.5	-0.5
n	2.655	2.820
a_1	0.001150	0.000215
η_1	0.420	0.686
κ	0.15	0.22

composite material. Degree of correlation in modeled and observed behavior of unreinfoced composite specimen are 98.1 %, 99.4 % and 99.9 % for confining pressure of 50, 100 and 200 kPa respectively. In the case of geogrid reinforced specimen the degree of correlation between modeled and experimentally observed results are 98.7, 99.7 and 99.9 % for confining pressure of 50, 100 and 200 kPa respectively. Hence justifying the statement that modeled behavior is good harmony with the experimentally observed behavior under triaxial loading.

9. REFERENCES

1. Yang, Z., "Strength and deformation characteristics of reinforced sand", PhD. thesis, University of California, Los Angeles, USA, (1972).
2. Kamel, M. A., Chandra, S. and Kumar, P., "Behaviour of Subgrade Soil Reinforced with Geogrid", ***International Journal of Pavement Engineering***, Vol. 5, No. 4, (2004), 201-209.
3. Abu-Farsakh, M. Y., Nazzal, M. D. and Louay, M., "Effect of Reinforcement on Resilient and Permanent Deformation of Base Course Material (07-0051), 86th TRB Annual Meeting, (2007).
4. Hausmann, M. R., "Strength of reinforced soil", ***Proc. 8th Australian Road Board Conf.***, Vol. 8, No. 13, (1976), 1-8.
5. Broms, B. B., "Triaxial Tests With Fabric Reinforced Soil", Proc. Int. Conf. on the use of fabric in geotechnics, Paris, (1977), 129-133.
6. Rao, G. V., Gupta, K. K. and Kachhawah, R., "Triaxial behavior of geotextile reinforced sand", ***Proc. Indian Geot. Conf***., Bangalore, India, Vol. 1, (1987), 323-328.
7. Baykal, G., Guler, E. and Akkol, O., "Comparison of woven and non-woven geotextile reinforcement using stress path tests", ***Proc. Int. sym. on Earth Reinforcement***, Kyushu, Japan, (1992), 23-27.
8. Soni, K. M., "Constitutive modelling of reinforced soil", PhD. Thesis, Indian Institute of Technology, Delhi, India, (1995).
9. Hausmann, M. R., "Geotextiles for unpaved roads-A review of design procedures", ***Geotextiles and Geomembranes***, Vol.5, (1987), 201-223.
10. Barenberg, E. J., Dowland, J. H. Jr. and Hales, J. II., "Evaluation of soil-aggregate systems with mirafi fabric", Department of Civil Engineering. University of Illinois, (1975).
11. Steward, J., Williamson, R. and Moheny, J., "Guidelines for use of fabric in construction of low-volume roads", USDA, Forest Service, Portland, Oregon, (1977).
12. Webester, S. L. and Watkins, E. J., "Investigation of construction techniques for tactical bridge approach roads across soft ground", Technical Report S-77-1, US Army Engineers, Waterways Experiment Station, Vicksburg, Miss, (1977).
13. Kinney, T. S., "Fabric induced changes in high deformation soil-fabric-aggregate systems", PhD. Thesis, Graduate College, University of Illinois, Urbana, USA, (1979).
14. Barenberg, E. J., "Design procedures for soil-fabric-aggregate systems with mirafi 500x fabrics", University of Illinois at Urbana: Champaign.
15. Giroud, J. P. and Noiray, L., "Geotextile reinforced unpaved road design", ***Proc. ASCE Jn. Geotechnical Engineering Div***., Vol. 107, No. GT9, (1981), 1233-1254.
16. Raumann, G., "Geotextiles in unpaved roads: design considerations", ***Proc. 2nd Int. Conf. on Geotextiles***, Las Vegas, USA, Vol. 2, (1982), 417-422.
17. Haliburton, T. A. and Barron, J. V., "Optimum depth method for design of fabric reinforced unsurfaced roads. Presented at the Annual Meeting", Transportation Research Record Board, (1983).
18. Barksdale, R., Robnett, Q., Lai, J. and Zeevaert-Wolff, A., "Experimental and theoretical behavior of geotextile reinforced aggregate soil systems", ***Proc. 2nd Int. Conf. on Geotextiles***, Las Vegas, USA, Vol. 2, (1982), 375-380.
19. Kinney, T. C., "Small scale load test on a soil-geotextile-aggregate system", ***Proc. 2nd Int. Conf. on Geotextiles***, Las Vegas, USA, Vol. 2, (1982), 405-409.
20. Douglas, R. A. and Kelly, M. A., "Geotextile reinforced unpaved logging roads: the effect of anchorage", ***Geotextiles and Geomembranes***, Vol. 4, (1986), 93-106.
21. Omoto, S., Kawabata, K. and Mizobuchi, M., "Reinforcement effect of geotextiles on pavement with weak subgrade", Earth Reinforcement Practice: Eds.

Ochiai, Hayashi and Otani. Rotterdam: Balkema, (1992), 671-676.

22. Desai, C. S., "A general basis for yield, failure and potential functions in plasticity", ***Int. J. Num. Anal. Meth. Geomech***., Vol. 15, No. 9, (1980), 649-680.
23. Desai, C. S., Somasundaram, S. and Frantziskonis, G., "A hierarchical approach for constitutive modelling of geologic materials", ***Int. J. Num. and Analytical Methods in Geomech.***, Vol. 10, (1986), 225-257.
24. Varadarajan, A. and Desai, C. S., "Material constants of a constitutive model determination and use", ***Indian Geotech. J***., Vol. 23, No. 3, (1993), 291-313.
25. Desai, C. S., "Hierarchical single surface and the disturbed state constitutive models with emphasis on geotechnical applications", Geotech. Eng. Emerging Trends in Design and Practice, Chap. 5, K. R. Saxena (Editor), New Delhi, India. Oxford and IBH Pub. Co. P·t. Ltd, (1994).
26. Aggarwal, Praveen, "Numerical modeling of geogrid reinforced unpaved flexible pavement", PhD. Thesis, Civil Engg. Dept., Indian Institute of Technology Delhi, New Delhi, India, (2002).
27. Aggarwal Praveen, "Modeling of water bound macadam behavior under triaxial loading using HISS model", Highway Research Bulletin, Indian Road Congress, New Delhi, India, No. 73, (2005), 37-48.
28. Wathugala, G. W., "Finite element dynamic analysis of nonlinear porous media with applications to piles in saturated clays", PhD. dissertation, Univ. of Arizona, Tuscan, Ariz., (1990), 187-194.
29. IRC: 19-1977, "Standard specification and code of practice for water bound macadam", The Indian Road Congress, New Delhi, India, (1982).
30. ASTM: D4595-86, "Test method for tensile properties of geotextiles by wide width strip method", ASTM standard of geotextiles, ***ASTM***, Philadelphia, PA, USA, (1988), 63-66.
31. Bishop, A. W. and Henkel, D. J., "The measurement of soil properties in the triaxial test", Edward Arnold Publishers ltd., London, (1962).